

Research on PMSM Speed Control of Rotary Steerable System based on Modified LADRC

Xi Zhou^a

School of Xi'an Shiyou University, Xi'an 710065, China

^azhouxi2650@163.com

Abstract

In response to the complex working conditions of the permanent magnet synchronous motor in the rotary steerable system under multiple sources of disturbance, the traditional Linear Active Disturbance Rejection Control(LADRC) has a large observation burden, hysteresis, and low accuracy due to significant load changes, which affects the adjustment of the drilling tool face angle and trajectory stability. Based on the permanent magnet synchronous motor (PMSM) speed current dual closed-loop vector control system, this paper introduces a disturbance observer to optimize the observation mechanism on the basis of the speed loop LADRC, and proposes an modified LADRC(MLADRC) speed control strategy. A simulation model of underground PMSM speed regulation was built in MATLAB/Simulink, and a comparative simulation was carried out under the conditions of speed step and load sudden changes of different amplitudes. The results showed that the designed disturbance observer could accurately capture load torque sudden changes. MLADRC achieved 0 overshoot under speed step and steady-state error control within ± 1 RPM. During load sudden changes of 5N·m and 15N·m, the speed fluctuation was smaller, the recovery time was shorter, and the anti-interference performance was better, which is suitable for underground load fluctuation scenarios. The MLADRC proposed in this article effectively solves the observation lag problem of traditional LADRC, providing a feasible solution for the optimization of PMSM speed regulation and the improvement of drilling trajectory stability in rotary directional drilling systems.

Keywords

Rotary Steerable System; Permanent Magnet Synchronous Motor; Linear Active Disturbance Rejection Control; Disturbance Observer.

1. Introduction

Petroleum, as a core strategic resource supporting the development of China's national economy and ensuring national energy security, is gradually shifting its exploration and development focus to deep and unconventional oil and gas fields, which puts strict requirements on the control accuracy, adaptability to working conditions, and anti-interference performance of drilling equipment[1]. As a core technology to break through the bottleneck of complex oil and gas reservoir development, the precise control of the tool face angle directly determines the accuracy of the drilling trajectory and is the key to achieving efficient development of unconventional oil and gas[2]. As the core driving unit of the Rotary Steerable System bias mechanism, the speed control performance of the downhole PMSM is the core element to ensure the precise adjustment of the tool face angle, which is directly related to the stability and efficiency of drilling operations.

The underground working environment is characterized by high temperature and pressure, strong vibration, and variable formation lithology, which makes the underground PMSM always face multi-source composite disturbances. The traditional speed control strategy is difficult to adapt to the strong disturbance and time-varying working conditions underground, and is prone to problems such as lagging speed control and insufficient anti-interference ability, which can lead to drilling trajectory deviation from the design track.

To solve the control disturbance problem under complex working conditions, researcher Han Jingqing proposed the ADRC algorithm. This algorithm abandons the dependence on the precise mathematical model of the controlled object, and estimates and compensates for the comprehensive disturbances inside and outside the system in real time by expanding the state observer[3]. With the advantages of simple structure and strong anti-interference ability, it has been widely used in the field of motor speed control. Among them, LADRC linearizes and simplifies ADRC, balancing control effectiveness and engineering feasibility, becoming the preferred solution for underground PMSM speed control[4]. The core of LADRC is the LESO, which needs to simultaneously estimate comprehensive disturbances such as motor speed, parameter perturbations, and load disturbances[5]. However, under the condition of significant load changes underground, the observation burden of a single LESO is significantly increased, which can lead to problems such as delayed disturbance estimation and decreased accuracy, resulting in limited compensation effect and restricting the overall control performance of LADRC[6].

In response to the shortcomings of traditional LADRC in the speed control of downhole PMSM in rotary directional drilling systems, this paper focuses on the high-performance speed control requirements of downhole PMSM, with the core of improving disturbance estimation accuracy and real-time performance. Based on traditional LADRC, an improved LADRC speed control strategy is proposed to solve the problem of observation lag under large load changes by optimizing the disturbance observation mechanism and sharing the observation burden of LESO[7]. Based on the MATLAB/Simulink simulation platform, a simulation model of underground PMSM speed control is built, and typical underground working conditions such as speed step and load mutation of different amplitudes are designed. Comparative simulation experiments are conducted between improved LADRC and traditional LADRC to verify the effectiveness and superiority of the improved strategy from the dimensions of dynamic response, anti-interference performance, and control accuracy. The aim of this study is to provide feasible solutions for optimizing the speed control of PMSM in rotary directional drilling systems, improving the precision of tool face angle control and drilling trajectory stability, and providing technical support for the efficient exploration and development of unconventional oil and gas resources in China.

2. Model and Vector Control System of PMSM

2.1 Mathematical Modeling of PMSM

This paper takes the surface-mounted three-phase permanent magnet synchronous motor as the research object, adopts the vector control with $i_d=0$, and establishes the mathematical model of the permanent magnet synchronous motor in the d-q coordinate system. The stator voltage equation is shown as equation (1):

$$\begin{cases} u_d = R_s i_d + L_s \frac{di_d}{dt} - \omega_e L_s i_q \\ u_q = R_s i_q + L_s \frac{di_q}{dt} + \omega_e L_s i_d + \omega_e \psi_f \end{cases} \quad (1)$$

where, u_q 、 u_d 、 i_q and i_d represent the voltage and current components of the stator on the d-q axis, respectively. R_s represents the stator resistance, L_s represents the stator inductance, ω_e represents the angular velocity, and ψ_f represents the magnetic flux of the permanent magnet.

The electromagnetic torque equation and mechanical motion equation are shown in equations (2) and (3):

$$T_e = 1.5 p_n \psi_f i_q \tag{2}$$

$$\dot{\omega}_m = \frac{3 p_n \psi_f}{2J} i_q - \frac{B \omega_m}{J} - \frac{T_L}{J} \tag{3}$$

where, J is the moment of inertia of the motor shaft end, ω_m is the mechanical angular velocity, T_L is the load torque applied to the motor, and B is the total friction coefficient experienced by the motor.

2.2 PMSM Vector Control System

The block diagram of the vector control system for permanent magnet synchronous motor is shown in figure 1. The system adopts a speed current dual closed loop architecture, where the speed outer loop takes the deviation between the set speed and the measured speed of the rotary transformer as input, generates a compensation signal through the speed loop regulator (ASR), and outputs the q-axis current reference value. The deviation between the reference value and the current sampling feedback signal is input into the current inner loop, and after being calculated by the current loop regulator (ACR), the output is converted into a voltage command in a stationary coordinate system through a coordinate transformation module.

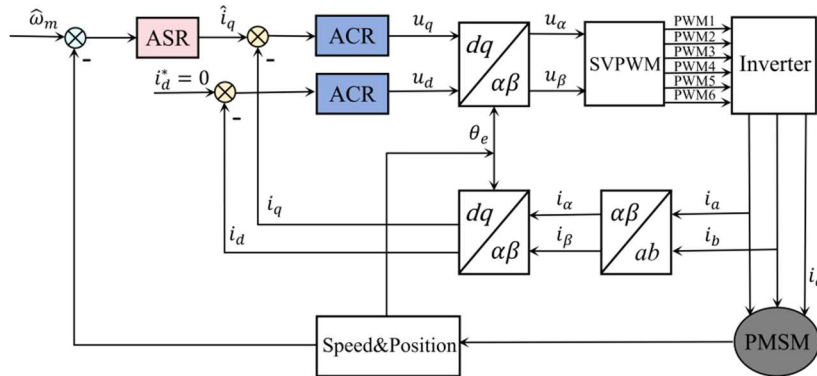


Figure 1. Block Diagram of PMSM Vector Control System

3. Design of Speed Loop Active Disturbance Rejection Controller

Based on the mechanical motion equation of permanent magnet synchronous motor, considering parameter perturbation and load disturbance, the mechanical motion equation can be expressed as:

$$(J_0 + \Delta J) \frac{d\omega_m}{dt} = (K_{t0} + \Delta K_t) i_q - T_L - (B_0 + \Delta B) \omega_m \tag{4}$$

where, J_0 , K_{t0} , and B_0 are the nominal reference values for moment of inertia, torque coefficient, and viscous friction coefficient, respectively; ΔJ , ΔK_t , and ΔB correspond to the nominal error values of

the above parameters under operating conditions. Introducing the q-axis current reference value, the equation can be further expressed as:

$$\frac{d\omega_m}{dt} = f(t) + b_0 \hat{i}_q \quad (5)$$

where, $b_0=K_{t0}/J_0$ is the nominal gain of the system; $f(t)$ is the total disturbance term of the speed loop, which includes the effects of internal parameter changes, sudden load torque, etc.

According to the LADRC design principle, selecting the state variable $x_1=\omega_m$ and extending the total disturbance $f(t)$ of the velocity loop to a new state variable x_2 , the velocity state equation can be expressed in the following form:

$$\dot{x}_1 = x_2 + b_0 \hat{i}_q \quad (6)$$

where, the controller gain is $b_0=1.5p_n\psi_f J$.
LESO can be expressed as:

$$\begin{cases} e_1 = z_1 - x_1 \\ \dot{z}_1 = z_2 - \beta_1 e_1 + b_0 \hat{i}_q \\ \dot{z}_2 = -\beta_2 e_1 \end{cases} \quad (7)$$

where, z_1 is the observed value of x_1 , and z_2 is the observed value of the total disturbance $f(t)$; e_1 is the observation error of rotational speed; β_1 and β_2 are LESO observation gains.

After disturbance compensation, the velocity loop can be approximately equivalent to a pure integral loop, so LSEF adopts proportional control. The final output control quantity is:

$$\begin{cases} u_0 = k_p (\hat{\omega}_m - z_1) \\ \hat{i}_q = (u_0 - z_2) / b_0 \end{cases} \quad (8)$$

where, k_p is the proportional gain; ω_m is the given velocity value.

According to the principle of pole placement, the poles of LSEF are placed at $-\omega_c$, where $\omega_c > 0$ is the closed-loop bandwidth of the velocity controller. From this, the controller gain can be obtained:

$$k_p = \omega_c \quad (9)$$

4. Improved Design of Speed Loop Self Disturbance Rejection Controller

In this study, the LESO of the velocity loop has the ability to observe the total disturbance of the system. To further improve the ability to observe load disturbances, this paper introduces a disturbance observer to share the observation burden of LESO. This method is based on the direct derivation of the mechanical motion equation of the motor, and has good real-time performance and engineering practicality.

The expression for the total disturbance $f(t)$ is:

$$f(t) = \frac{d\omega_m}{dt} - b_0 \hat{i}_q \quad (10)$$

To suppress the interference of measurement noise caused by speed differentiation on disturbance observations, a first-order low-pass filter $L(s)$ is introduced:

$$L(s) = \frac{1}{\tau_0 s + 1} \quad (11)$$

where, τ_0 is the time constant of the low-pass filter, used to strike a balance between observed response speed and noise suppression. After substituting the filtering process, the observed value of the total disturbance can be obtained:

$$\hat{f}(s) = \frac{\frac{\omega_m(s)}{\tau_0}(\tau_0 s + 1) - (\frac{\omega_m(s)}{\tau_0} + b_0 \hat{i}_q)}{\tau_0 s + 1} = \frac{\omega_m(s)}{\tau_0} - \frac{\frac{\omega_m(s)}{\tau_0} + b_0 \hat{i}_q}{\tau_0 s + 1} \quad (12)$$

The structural diagram of the disturbance observer is shown in the following figure 2. This structure integrates the information of rotational speed ω_m and q-axis current, and outputs disturbance observation values after low-pass filtering, achieving integrated observation of time-varying disturbances such as load disturbances.

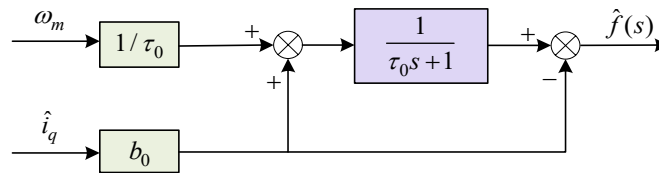


Figure 2. Block Diagram of Disturbance Observer Structure

If the disturbance amount estimated by the disturbance observer is fed forward to LESO as a known disturbance, the improved LESO expression is adjusted to:

$$\begin{cases} e_1 = z_1 - x_1 \\ \dot{z}_1 = z_2 - \beta_1 e_1 + b_0 \hat{i}_q + \hat{f}(t) \\ \dot{z}_2 = -\beta_2 e_1 \end{cases} \quad (13)$$

If the control law still adopts proportional control, the output control quantity is:

$$\begin{cases} u_0 = k_p (\hat{\omega}_m - z_1) \\ \hat{i}_q = (u_0 - \hat{f}(t) - z_2) / b_0 \end{cases} \quad (14)$$

This method only requires observation of residual disturbances, significantly reducing the observation burden of LESO, improving the accuracy and real-time performance of disturbance observation, and thereby enhancing the overall control performance of the active disturbance rejection controller.

5. Simulation Analysis

Build a simulation model of permanent magnet synchronous motor speed vector control on MATLAB/Simulink simulation platform. Based on this simulation model, comparative simulation experiments were conducted, selecting LADRC speed controller and the MLADRC speed controller designed in this paper for performance comparison. During the experiment, a PI controller was uniformly used as the current loop control strategy. The main parameters of the permanent magnet synchronous motor used in this article are shown in Table 1.

Table 1. Parameters of PMSM

Parameter	Symbol	Value	Unit
Pole Pairs	P_n	6	
Stator Resistance	R_s	1.11	Ω
Stator Inductance	L_s	0.008	H
Permanent Magnet Flux Linkage	ψ_f	0.225	Wb
Moment of Inertia	J	0.003	$\text{kg}\cdot\text{m}^2$

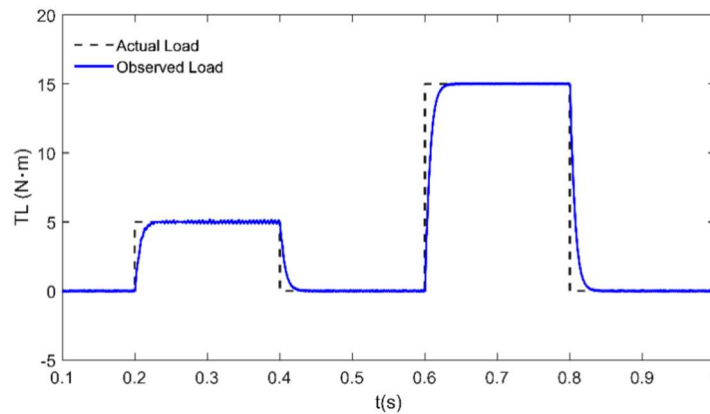


Figure 3. Observation Results of Load Torque

Design the following simulation conditions: set the motor speed to be constant, the initial load torque to 0, suddenly add 5N·m load at 0.2s, suddenly reduce to no load at 0.4s, suddenly add 15N·m load again at 0.6s, and restore to no load at 0.8s. Ignore the influence of the viscous friction coefficient B during the simulation process and eliminate irrelevant factors. The load disturbance observed by the disturbance observer designed in this article is $-T_L/J_0$. In order to facilitate intuitive comparison with the actual load torque, the output result of the disturbance observer is multiplied by $-J_0$ in the simulation for conversion processing. The specific observation result of the disturbance observer on the load torque is shown in figure 3. Regardless of whether the load torque is in a sudden increase or

decrease stage, the observed value of the load torque output by the observer can respond quickly and almost completely coincide with the actual load torque curve. This fully validates the precise capture ability of the disturbance observer for load torque disturbances.

Design speed step simulation conditions under no-load start-up: The motor is initially started under no-load, and the speed command is set to 60RPM at $t=0s$. The step jumps to 180RPM at $t=0.2s$, continues to jump to 300RPM at $t=0.4s$, and drops to 100RPM at $t=0.6s$. Based on this operating condition, test the performance of LADRC speed controller and MLADRC speed controller separately. The no-load speed regulation curve is shown in the figure 4.

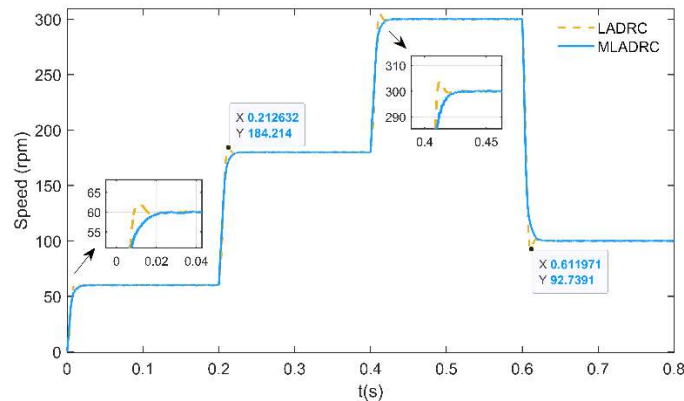


Figure 4. Speed Following Performance Response Curve

During the no-load start-up and speed increase stages, the overshoot of the conventional LADRC is 4.1%, while the MLADRC maintains 0 overshoot during both speed increase processes. The steady-state error of the final speed is controlled within $\pm 1RPM$, meeting the requirements of the speed steady-state accuracy index. In the step down stage of speed reduction, under conventional LADRC control, the speed drops to 92.74 RPM, while MLADRC relies on load disturbance compensation to significantly reduce the amplitude of speed drop, and the dynamic tracking process is closer to the target speed, reflecting its dynamic stability advantage under variable speed conditions.

Set the motor to maintain the target speed command at 120RPM after starting with no load, suddenly increase the load by $5N \cdot m$ at $t=0.2s$, and suddenly decrease the load by $5N \cdot m$ to no load at $t=0.4s$; Subsequently, at $t=0.6s$, a load of $15N \cdot m$ was suddenly added, and at $t=0.8s$, a load of $15N \cdot m$ was suddenly reduced to no load. Based on this operating condition, the speed response characteristics of LADRC and MLADRC speed controllers were tested separately, and the corresponding response curves are shown in the figure 5.

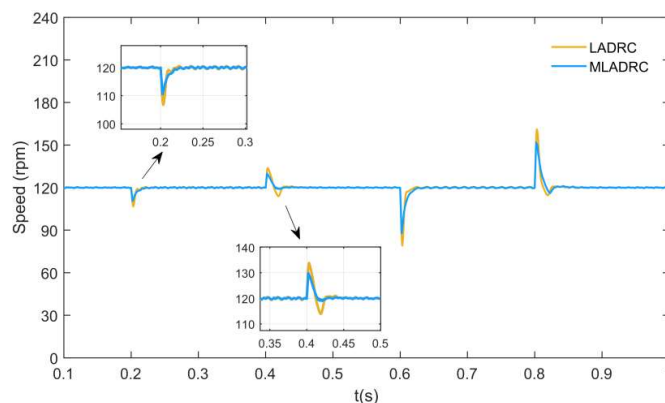


Figure 5. Speed Anti-interference Performance Response Curve

Under the condition of a sudden load change of $5\text{N}\cdot\text{m}$, the dynamic speed drop of the LADRC controller is 106.77RPM , the recovery time is 7ms , and the steady-state error is reduced to 0.16% ; MLADRC relies on disturbance compensation to increase the dynamic speed drop to 110.54RPM , shorten the recovery time to 6.5ms , and make the speed closer to the target value of 120RPM , resulting in better timeliness and stability of anti-interference response. Under the load mutation condition of $15\text{N}\cdot\text{m}$, the dynamic speed drop of conventional LADRC is 79.14RPM , with a recovery time of 8.6ms ; the dynamic speed drop of MLADRC is increased to 87.97RPM . The MLADRC controller further reduces the amplitude of speed fluctuations during sudden load changes, shortens the recovery time, and improves the anti-interference performance in a targeted manner, making it more suitable for load fluctuation scenarios caused by sudden changes in the lithology of underground formations.

6. Conclusion

This article takes the surface mounted three-phase permanent magnet synchronous motor as the research object. In response to the problem of insufficient observation disturbance ability of conventional LADRC under sudden changes in underground load in $i_d=0$ vector control, an MLADRC integrating disturbance observer is designed, which effectively improves the accuracy and real-time performance of disturbance observation. MATLAB/Simulink multi condition simulation verification shows that the designed disturbance observer can capture sudden changes in load torque, and MLADRC achieves zero overshoot and significant reduction in deceleration drop amplitude during speed step conditions, with steady-state error controlled within $\pm 1\text{RPM}$; Under sudden load changes of $5\text{N}\cdot\text{m}$ and $15\text{N}\cdot\text{m}$ underground, compared to LADRC, this controller has smaller speed fluctuations, shorter recovery time, and improved anti-interference performance. This provides a reliable solution for the speed control of the underground permanent magnet synchronous motor drive system, and its design concept can also be extended to other PMSM speed control scenarios with high requirements for real-time control and anti-interference. In the future, the robustness of the controller can be further optimized based on the actual working conditions underground, and physical experiments can be carried out to promote its engineering application.

References

- [1] GAO Deli, HUANG Wenjun. Basic research progress and prospect in deep and ultra-deep directional drilling[J]. Natural Gas Industry, 2024, 44(1): 1-12.
- [2] QIN Yonghe, YANG Jianyong, FANG Pingliang, et al. Develop rotary steerable drilling; promote unconventional oil and gas revolution[J]. Petroleum Science and Technology Forum, 2025, 44(1): 43-50.
- [3] LIU C Q, LUO G Z, TU W C. Research review on active disturbance rejection control of permanent magnet synchronous motors for aerospace electromechanical actuators [J]. Journal of Electrical Engineering, 2021, 16 (4): 12-24.
- [4] YUAN H R, ZHOU F Q, SUN J H. Improved linear active disturbance rejection control method for permanent magnet synchronous motor based on load torque observer[J]. Electronic Measurement Technology, 2025, 48 (9): 36-43.
- [5] JIN H Y, ZHANG R Q, WANG L, et al. Root locus analysis of robustness for parameter tuning of linear active disturbance rejection control [J]. Control Theory & Applications, 2018, 35 (11): 1648-1653.
- [6] XU W B, WEI Z Y, KONG W, et al. Parameter tuning of linear active disturbance rejection controller for PMSM servo system [J]. Control Theory & Applications, 2022, 39 (1): 165-178.
- [7] QU LZH, QIAO W, QU L Y. Active-disturbance rejection-based sliding-mode current control for permanent-magnet synchronous motors[J]. IEEE Transactions on Power Electronics, 2021, 36(1): 751-760.